IEEE Access
Multidisciplinary ⋮ Rapid Review ⋮ Open Access Journal

Received February 4, 2022, accepted February 20, 2022, date of publication February 28, 2022, date of current version March 11, 2022.

*Digital Object Identifier 10.1109/ACCESS.2022.3155544*

# Development of Beam Steerable Reflectarray With Liquid Crystal for Both E-Plane and H-Plane

**XIAOTONG LI[1], (Student Member, IEEE), HIROYASU SATO[1], (Member, IEEE), YOSEI SHIBATA[2], TAKAHIRO ISHINABE[2], (Member, IEEE), HIDEO FUJIKAKE[2], (Senior Member, IEEE), AND QIANG CHEN[1], (Senior Member, IEEE)**

[1]Department of Communications Engineering, Graduate School of Engineering, Tohoku University, Sendai 980-8579, Japan
[2]Department of Electronic Engineering, Graduate School of Engineering, Tohoku University, Sendai 980-8579, Japan

Corresponding author: Xiaotong Li (li.xiaotong.r4@dc.tohoku.ac.jp)

This work was supported by the Ministry of Internal Affairs and Communications in Japan under Garnt JPJ000254.

**ABSTRACT** In this paper, a reconfigurable reflectarray (RA) with two-finger element composed of electrically biased liquid crystal (LC) at millimeter wave band is proposed. An orthogonal bias network is proposed and developed, which can result in changes in the equivalent relative permittivity of the liquid crystal, and reflection phase along direction $x$ and direction $y$ can be realized, thus beam steering at both E-plane and H-plane can be achieved. The LC RA is composed of 10 $\times$ 10 elements of 2-finger unit, a standard horn antenna is obliquely placed as feed, and radiation pattern is calculated by array synthesis and full wave simulation. It is found that beam scan at both E-plane and H-plane can be achieved. Compared with former researches of LC RA, this work introduces a simple scheme to achieve beam scan for LC RA at both E-plane and H-plane.

**INDEX TERMS** Reconfigurable, reflectarray, liquid crystal, beam scan.

## I. INTRODUCTION

Reflectarrays have attracted increasing attention over the past years because of their unique properties: low loss due to the absence of a corporate feed, ease of fabrication, planarity and low weight and lower cost [1], [13]. Reconfigurability, a generally highly desirable feature, would increase their versatility even more. The previous works on RAs are mainly focused on the unit design [2]–[5] and generating a fixed pattern optimized by algorithm [6]–[11]. Many of these works are about influence of unit parameters on phase change and fixed element distribution on the array [2]–[10].

Recently, efforts are devoted to the realization of dynamicly reconfigurable reflection units [11]. In fact, based on the known properties of changing reflection phase with different methods on RA, dynamically controllable reflected wave gets the most notice [1]. In the field of real-time control, various technologies especially electronic control approaches to realize reconfigurability are getting more and more attention, such as ferroelectric thin films, varactor diodes [13], RF MEMS [14]–[17], mechanical rotation [14], LC [18]–[25] and so on. However, loss of ferroelectric flms at millimeter wave band can not be ignored. Besides the high costs, MEMS and diodes integrated on RA also have the problem of assembling. Contrarily, LC is low cost and easily integrated to antennas and microwave devices with planar structures, which is suitable to be assemble to the RA. As a result, studies of LC applications on RA technology at millimeter wave have increased a lot [22], [26]–[29].

The LC RA usually uses the material properties that can change relative permittivity by adding quasi-static electric field to the electrodes [22], [34]. When different voltages are applied to the Patch layer of RA relative to the ground, phase with different values of reflected wave from the RA is achieved.

The previous design of the LC RA unit mainly used thin-line electrodes to connect the patch layer [21]–[25], so these RA can just steer beam in one plane [21]. A solution to achieve beam steer at two orthogonal planes is proposed in [35], but it needs many bias lines, another scheme is came up to achieve beam shift at E-plane and H-plane with concept of subarray and the contorl of bias lines [36], which is a significant improvement of LC RA. Base on the idea of bias lines and detialed investigation of distribution of liquid crystal molecules in a three-dimensional environment, this paper proposes a simpler solution to achieve beam steering at

The associate editor coordinating the review of this manuscript and approving it for publication was Mengmeng Li.

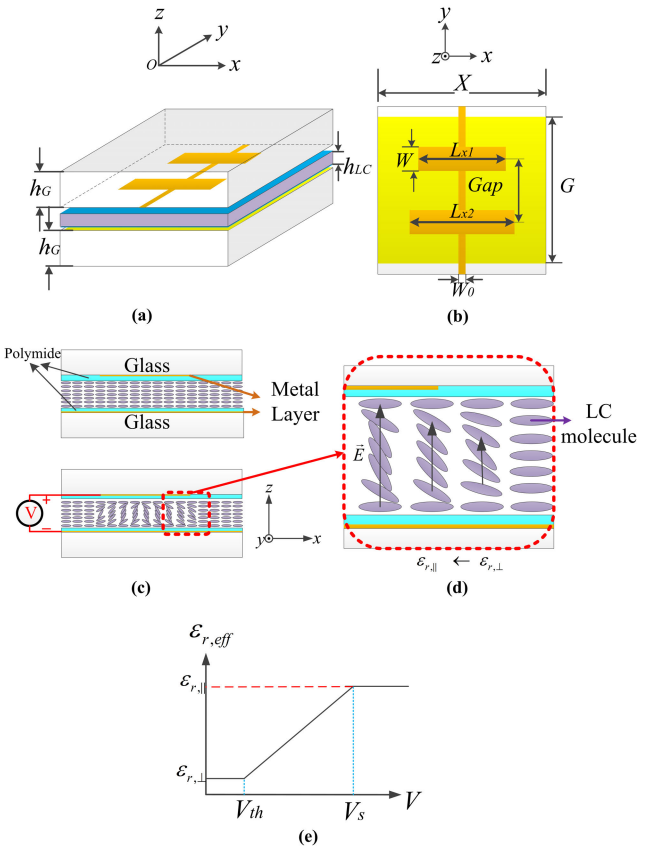


**FIGURE 1.** Geometry of the LC RA unit. (a)3D view of LC RA unit; (b) Top view of LC RA unit; (c) The LC molecules distribution in RA when the unit is w/o biased and biased; (d) Detailed LC molecules distribution when the RA unit is biased; (e) Relationship of relative permittivity and bias voltage.

both E-plane and H-plane by discrete ground and cross bias condition, which is more practical in engineering.

This article is organized as follows: Section II presents the multi-resonant RA unit structure 2-finger and discrete ground, explains the working principles, the ability of this RA unit to change the phase and amplitude of the reflected wave is discussed, and the characteristics of the reflected wave changing with the liquid crystal state under a certain incident angle is mimiced. Section III introduces the bias network and priciples that can steer LC molecules at two directions, which change the phase of RA at both E-plane and H-plane, this application on array that can achieve beam steering by analysis of both array synthesis and full wave synthesis, the performance of the LC RA (Beam scanning at both E-plane and H-plane) with different bias conditions are shown. Section IV concludes this paper.

## II. DESIGN OF LC RA ELEMENT

Here a 2-finger structure shown in Fig.1 is used as unit of LC RA. This multi-resonant element appllicaiton in LC RA unit is firstly presented in [28], which can achieve reflection phase change, this structure exhibits excellent performance of reflection phase variation more than 330° within a broad

**TABLE 1.** Unit parameters.

| Variable | Numerical Values (mm) | Variable | Numerical Values (mm) |
|---|---|---|---|
| $h_G$ | 0.60 | $h_{LC}$ | 0.25 |
| $X$ | 4.00 | $Gap$ | 2.00 |
| $G$ | 3.95 | $W$ | 0.30 |
| $L_{x1}$ | 1.95 | $W_0$ | 0.20 |
| $L_{x2}$ | 2.20 | | |

frequency. In this work, Particle Swarm Optimization (PSO) is applied to develop and optimize the parameters of this structure to achieve larger phase shift range over 360° and relative high reflection coefficient, which are two basic indexes for RA element design. The liquid crystal used in the design is LC-BYE7, its material parameters are used as follows: relative dielectric constant changes from $\varepsilon_{r,\perp} = 2.1$ to $\varepsilon_{r,//} = 3.2$, loss tangent varies from $\tan\delta_\perp = 0.014$ to $\tan\delta_{//} = 0.004$, and these parameters have been tested in [35], and relative permittivity increase with bias voltage increase [37].

This element uses traditional sandwich structure shown in Fig. 1, there are five layers in the structure of LC RA unit: the top layer is the quartz glass ($\varepsilon_r = 3.2$, $\tan\delta = 0.002$), the second layer is the patch layer, the third layer is the sealed LC, the fourth layer is the metalized ground layer, the bottom layer is also quartz glass. The parameters of the LC RA are marked at the Fig. 1(a) and Fig. 1(b), by simulation of electromagnetic software Ansys HFSS and optimization algorithm, proper values of the parameters are chosen in the Table 1, different from the original model 2-fringer structure presented in [28], a slot on the bottom metal layer of glass is attached to separate the ground in the direction $y$ which is orthogonal to the path layer.

In simulation model of HFSS, the metal layer is chosen as the the same material properties as copper with thickness of 5 $\mu$m, which is numerically greater than the skin depth at the target frequency 37.5 GHz, and the ploymide of 0.9 um along direction $x$ is attached on the surface of the glass, which can guarantee the initional directions of the rod-shaped LC molecules (Fig. 1(c) and Fig. 1(d)), and the incident wave travelling along $-z$ direction would respond differently when LC is biased with different quasi-static vlotages. To mimic the procedure of bias voltage applied to the LC, which is illustrated in Fig. 1(e), relative permittivity increase from $\varepsilon_{r,\perp}$ to $\varepsilon_{r,//}$ almost linearly when bias voltage increase from the threshold voltage $V_{th}$ to satruated voltage $V_s$, which is tested in [37]. Linear variation of LC changing from $\varepsilon_{r,\perp} = 2.1$, $\tan\delta_\perp = 0.014$ to $\varepsilon_{r,//} = 3.2$, $\tan\delta_{//} = 0.004$ is applied in the simulation model at frequency band from 30 GHz to 48 GHz. The simulation results are shown in Fig. 2, the magnitude of the reflected wave from RA is shown in Fig. 2(a), the return loss changes from $-0.25$ dB to $-2.10$ dB at the band from 33.0 GHz to 42.0 GHz, which is relatively low loss compared with other LC RAs. The phase is shown in Fig. 2(b), the phase steering scale of more than 360° is achieved at the frequency band from 37.2 GHz to 38.0 GHz.

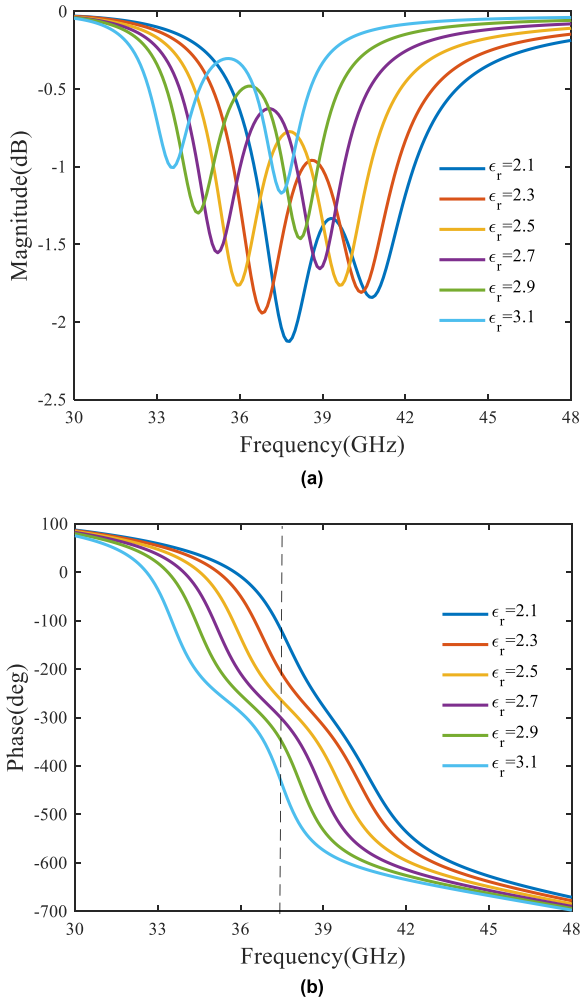


**FIGURE 2.** Simulation of Reflection Coefficient from LC RA unit in floquet mode when different bias voltage is applied. (a) Magnitude of the Reflection Coefficient as a function of frequency when LC is biased with different voltage and appear different relative permittivity; (b) Phase of the Reflection Coefficient as a function of frequency when LC is biased with different voltage and appear different relative permittivity.

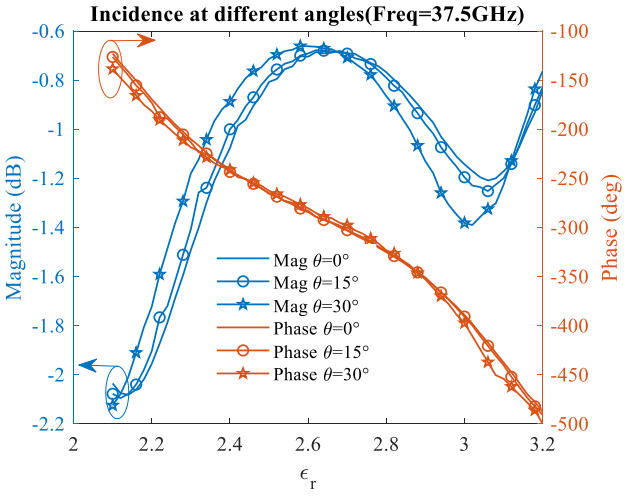


**FIGURE 3.** Magnitude and phase of reflection coefficient from LC RA with different incident angle at frequency 37.5 GHz.

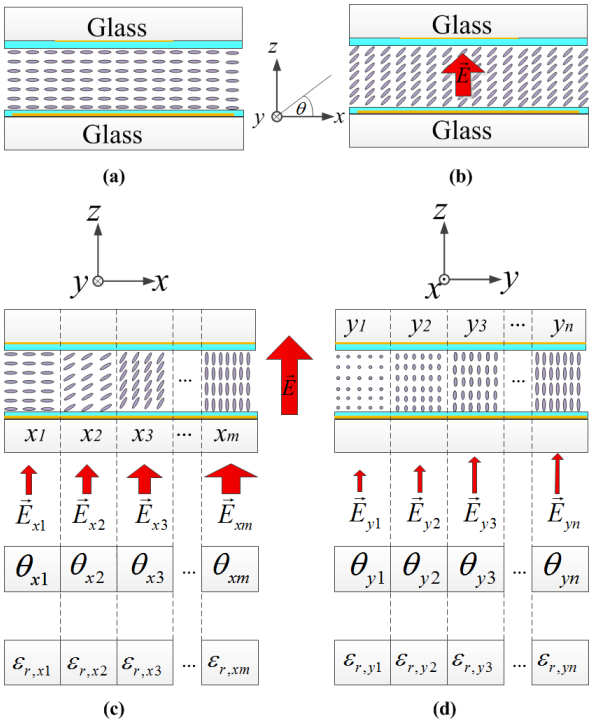


**FIGURE 4.** LC properties under DC voltage steering when glass is alignment along x direction. (a)Initial state of LC molecules w/o bias; (b)State of LC molecules w bias when rubbing is along x; (c)Relative permittivity distribution in xOz plane as different bias is added along x; (d)Relative permittivity distribution in yOz plane as different bias is added along y.

At the target frequency point 37.5 GHz, the magnitude and phase steering conditions of LC RA are presented in Fig. 3, the magnitude of scattering filed varies from −2.1 dB to −0.6 dB within the changing state of LC, and phase decrease from −123° to −488° as the relative permittivity increase, the phase steering scale is over 360° and can be utilized in the reconfigurable RA. Even when the incident angle is 0-30° with respect to the $-z$ axis, the amplitude of reflected wave is still above −2.2 dB, and the phase change is numerically greater than 360°, which is good index for RA design.

## III. LC RA INTEGRATION AND BIAS SCHEME FOR CONTROLLING RADIATION PATTERN

### A. LC PROPERTIES UNDER DC BIAS VOLTAGE

To achieve the stable reconfigurable performance, the directions of LC molecules should be guaranteed to keep the relative permittivity in a certain value (Fig. 4(a)), so rubbing procedure is needed. Usually, polymide is used as alignment film to cover the metal-side surface of glass [21], complicated heating process and rubbing procedure are required, here rubbing along direction $x$ is chosen, which allows the LC molecules to rotate with an angle $\theta$ relative to axis $x$ in $xOy$ plane (Fig. 4(b)). So if the ground layer of the RA is separated with slot along direction $x$, apply different voltages

to different parts of ground $x_1$, $x_2$, $x_3, \ldots, x_m$ relative to patch layer, different relative permittivity of LC in the RA unit appears (like Fig. 4(c)), so the RA unit can achieve phase controlled along direction $x$; if the patch layer of the RA is discretized with slot along direction $y$, apply different voltages to different parts of ground $y_1, y_2, y_3, \ldots, y_n$ relative to patch layer, different relative permittivity of LC in the RA unit is obtained (like Fig. 4(d)), so the RA unit can achieve phase controlled along direction $y$.

### B. DESIGN OF BIAS NETWORK FOR LC RA

To achieve the reconfigurable performance, Static driving voltage is usually used in the control LC modules because of its the stability and low-cost, so it is also common in LC RA. The LC RA usually connect the unit cell with a bias line in one direction, which is convenient for control, but this scheme to control the unit has limitations that just one line can be controlled by bias voltage. Even though some papers present some scheme of bias to achieve unit controlled more than one direction, however, it needs complex bias layout and with the number of units increasing, more bias lines are need. More bias lines would occupy to much space on the surface of the substrate surface of RA, which is destructive to the electromagnetic properties and performance of RA.

Based on the works and ideas from pervious scholars, the electrode is integrated on one line to connect the bias line, the phase of RA can be controlled by different bias voltages, this paper proposes a scheme of electrode connection: the finger structure are connected in one column by bias lines and the grounds are connected in one row, thus the phase of reflected wave from RA can be controlled in two mutually orthogonal directions (as shown in Fig. 5): when the voltage electrodes connected to the ground are set $V_{b1} = V_{b2} = V_{b3} = \cdots = V_b$, the voltage electrodes form DC voltage module connected to patch layer are set different values $V_{a1}$, $V_{a2}$, $V_{a3}, \ldots, V_{a10}$, so the phase of RA element can vary in direction $y$; if the voltage electrodes connected to the patch layer are the same $V_{a1} = V_{a2} = V_{a3} = \cdots = V_a$, and the discrete ground sections are biased with different voltages $V_{b1}, V_{b2}, V_{b3}, \ldots, V_{b10}$, the phase of RA element will change in direction $x$.

Considering the orthogonal bias network scheme, a RA with $10 \times 10$ elements is presented, where just 2 groups bias lines and total number 20 are distributed in both upper layer and the ground plane layer. By proper bias of one group electrodes the same voltage and another group with different values, orthogonal phase steering can be achieved thus beam steering at both E-plane and H-plane can be achieved.

### C. RADIATION PATTERN OF THE LC RA

The positional relationship between feed antenna and RA should be chosen carefully because it influences a lot on the system performance [38]. Large $F/D$ results in high illumination efficiency but cause high edge taper; small $F/D$ will increase the spillover efficiency and lower the edge taper of RA to ensure that more electromagnetic wave is utilized to generate a beam, so it is a tradeoff to choose $F$ when considering the efficiency even if the feed is placed at near field [38]. The feed antenna is usually placed at a certain angle off the $-z$ axis to eliminate feed blockage when the beam is scanning, meanwhile oblique incidence on RA appears, but it is acceptable if the oblique incident angle is small.

In this LC RA system, we set the coordinate origin locating at the center of RA, direction $x$ is along bias lines of patch layer, direction $y$ is along the dipole of RA unit. In order to get high apeture efficiency and low edger taper for the RA, $1.0 \leq F/D \leq 2.0$ is usually chosen for the RA system, and we would like to choose the value in this range within near filed but not too near. To avoid the obstacle problem of feed, we use a standard horn antenna working at Ka band with gain of 24.0 dBi as the feed and locate it at the coordinate (0.00, −34.64, 40.00) mm, which could provide an oblique incidence of 30° with polarization of TM mode (Fig. 5(a)). In this condition, the $10 \times 10$ elements RA has a aperture size of 40mm, $F/D$ =1.38, which can guarantee the high apearture efficiency. The radiation condition from antenna to RA at 37.5 GHz is shown in Fig. 6. Magnitude is shown in Fig. 6(a), the magnitude on the edege of RA is −11.0 dB which is an acceptable value for aperture antenna considering the edge tapper.

Since the normal form of horn antenna aperture is in $xOz$ plane and the E-plane of the feed is along the direction $y$, the co-polarization of the incident wave is direction $y$. Once the incident electric field componenets on the aperture of each element are computed, the reflected fields for each element in RA can be obtained by the generalized scattering matrix, which relates the field components of incident field and reflected field in periodic structure.

$$\begin{bmatrix} E_x^{ref}(m,n) \\ E_y^{ref}(m,n) \end{bmatrix} = \begin{bmatrix} \Gamma_{xx} & \Gamma_{xy} \\ \Gamma_{yx} & \Gamma_{yy} \end{bmatrix} \begin{bmatrix} E_x^{inc}(m,n) \\ E_y^{inc}(m,n) \end{bmatrix} \tag{1}$$

The space phase of the incident wave on each RA element can be obatined by the following equation

$$\phi_{psd} = -k_0 R_i \tag{2}$$

$R_i$ is the Euclidean distance from the phase center of the horn antenna to the RA element i, $k_0$ is the free space wave number, and the space phase distribution is shown in Fig. 6(b). Since all the elements of LC RA are the same, the phase of reflected wave of RA just has a phase shift of the space phase delay $\phi_0$, $\phi_{RA} = \phi_{psd} + \phi_0$. The phase of RA element can be used to calculate the pattern in the subsequent radiation pattern.

When the electrodes are biased with DC voltage with different values, the reflected wave from LC RA unit of different columns or rows will change with different phase $\phi_{LC}$,

$$\phi_{RA,mn} = -k_0 R_{mn} + \phi_0 + \phi_{LC,mn} \tag{3}$$

With array synthesis, the phase of one column or one row RA can be modulated by DC voltage, considering the radiation Pattern of 2-dimensional RA is summation of reflected

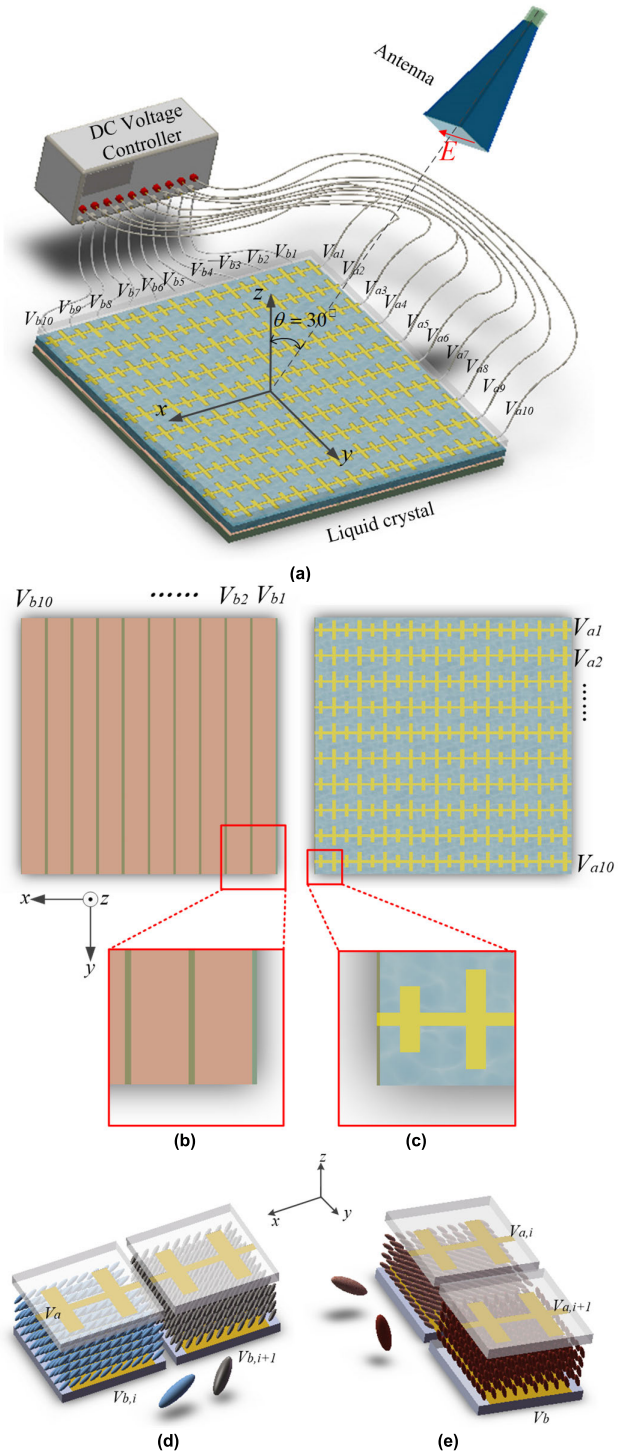


**FIGURE 5.** Geometry of the reconfigurable LC RA system. (a)3D view of LC RA system with orthogonal bias line. Top view of the LC RA: (b)Slots along direction y discrete the ground into 10 sections and voltages can add different values along direction x. (c) voltages can add different values along direction y (d)Details of LC molecules in the LC RA unit when different voltages are applied along y. (e) Details of LC molecules in the LC RA unit when different voltages are applied along x.

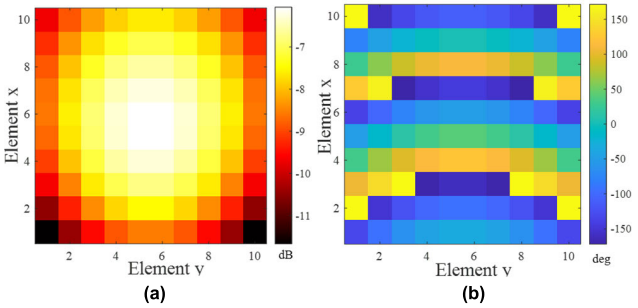


**FIGURE 6.** Magnitude of incident wave and space phase distribution on the RA at frequency 37.5GHz when horn antenna is used as feed. (a)Magnitude; (b) Phase.

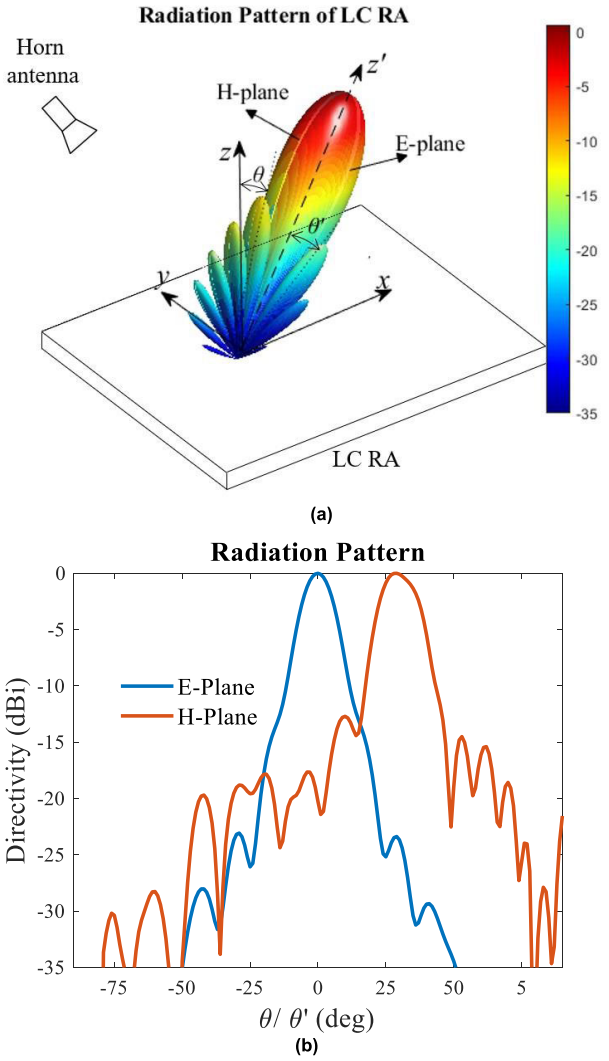


**FIGURE 7.** Radiation Pattern of LC RA. (a) 3D radiation pattern of LC RA; (b) Planner pattern of E-plane and H-plane for LC RA.

wave from each element,

$$\vec{E}(\hat{u}) = \sum_{m=1}^{M}\sum_{n=1}^{N} A_{mn}(\hat{u}) \cdot \vec{I}(\vec{r}_{mn}) \tag{4}$$

$$\hat{u} = \hat{x}\sin\theta\cos\phi + \hat{y}\sin\theta\sin\phi + \hat{z}\cos\theta \tag{5}$$

Here M is the number of column array along direction $x$, N is the number of row array along direction $y$; m and n are

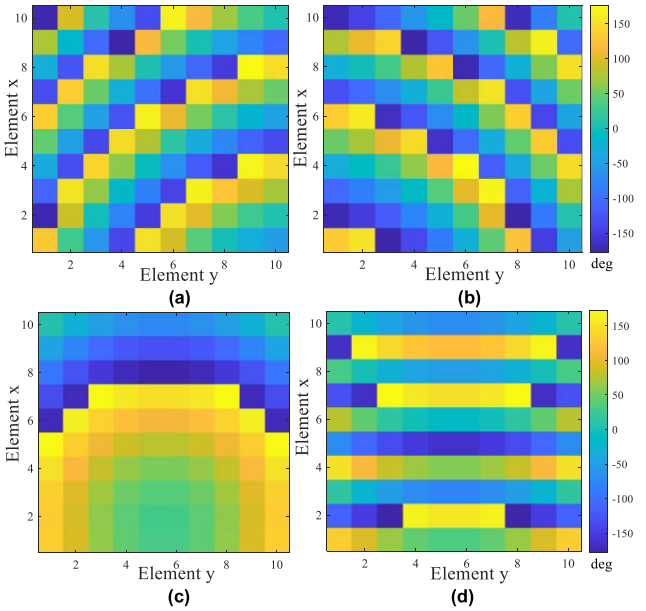


**FIGURE 8.** Phase steering of each element on LC RA. (a) Phase steering at +y direction; (b) Phase steering at −y direction; (c) Phase steering at −x direction; (d) Phase steering at +x direction.

the orders of the LC RA along directions $x$ and $y$; A is the RA element pattern function, using a scalar approximation of cosine $q_e$ model for the RA unit; The element excitation $I(r_{mn})$ is caused by the incident field and response properties of LC,

$$A_{mn}(\theta, \varphi) = \cos^{q_e}(\theta) \cdot e^{jk(\vec{r}_{mn} \cdot \hat{u})} \tag{6}$$

$$I_{mn} = E_y \Gamma_{yy} \cdot e^{j\varphi_{mn}} \tag{7}$$

Thus, the directivity D can be calculated by the definition and beam is shown in Fig. 7. The 3D polar pattern is shown in Fig. 7(a), the H-plane is $xOz$ plane, and E-plane is at $yOz'$ plane which inclined by 30° relative to the $yOz$ plane. The normalized E-plane and H-plane of the pattern are presented in Fig. 7(b), from which the maximum radiation at $\theta = 30°$, $\varphi = 0°$ can be observed, the sidelobe level of E-plane and H-plane is −23.0 dB and −12.5 dB, both of them are good indexes for antennas.

### D. STEER BEAM AT H-PLANE AND E-PLANE FOR LC RA

To steer beam at E-plane, progressive phase distributed on the plane perpendicular to $z$' is needed, so a scheme is provided: the voltage electrodes connected to the ground are the same value $V_b$, and the patch layers are biased with different voltages $V_{a1}, V_{a2}, V_{a3}, \ldots, V_{a10}$, the phase of reflected wave from each column along direction $y$ will be controlled, so the phase center of reflected wave will shift along direction $y$, an example of progressive phase difference of −60° and 60° for RA are shown in Fig. 8(a) and (b), thus the phase front will be steered in E-plane, progressive phase difference along $y$ will result in the beam direction normalized to the equal phase front and scanning in E-plane. The same requirements happen

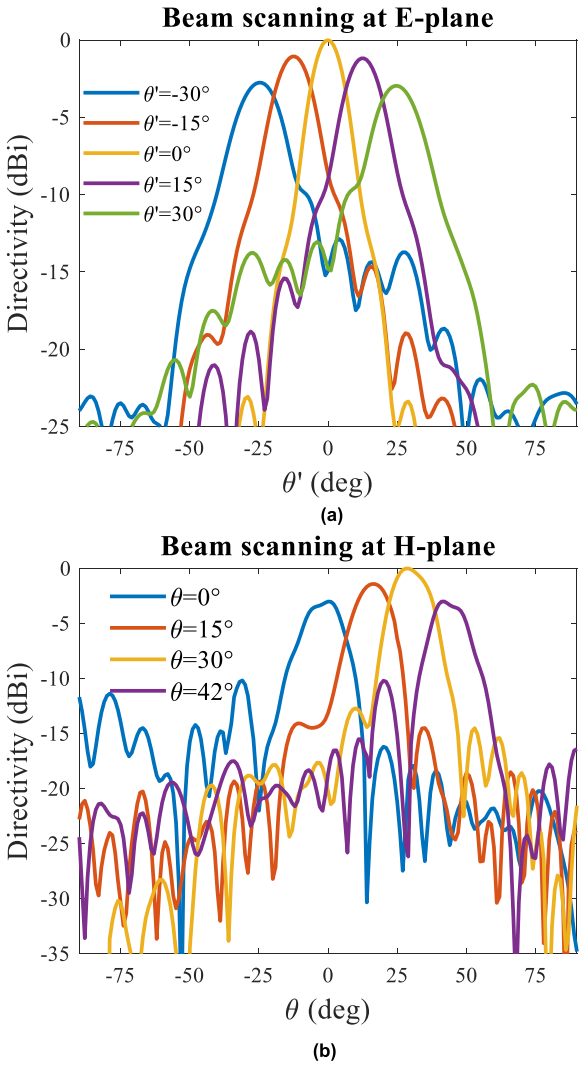


**FIGURE 9.** Beam scanning of LC RA. (a)Beam scanning at E-plane; (b)Beam scanning at H-plane.

for the beam steering at H-plane, but with a symmetrical DC bias scheme: that the patch layers are biased with the same value $V_a$, the ground are biased with different voltages $V_{b1}, V_{b2}, V_{b3}, \ldots, V_{b10}$, the phase of reflected wave from each row along direction $x$ can be changed according to the controlled $V_b$, so the phase center of reflected wave will shift along direction $x$, a comparison of progressive phase difference of −60° and 60° along direction $x$ at the RA aperture are shown in Fig. 8 (c) and Fig. 8(d), thus the phase front will be steered in H-plane, and beam can be steering in H plane. The prescribed relative permittivity of LC can be obtained by interpolation solution from Fig. 3(b), when relative permittivity is decided the magnitude respond can also be attained from Fig. 3(a).

When the electrodes on one side are biased the same voltage and steer voltage in the other side, orthogonal beam steering can be achieved, the performance of the LC RA can be computed by the array synthesis approach described in

the former section. And the calculated beams of the different bias conditions are shown in Fig. 9, the Fig. 9(a) exhibit the beam scanning properties at E-plane, from the figure, beam scanning angle $\theta$ relative to the axis $z'$ can cover from $-30°$ to $30°$, with the scanning angle increasing from center of E-plane $z'$, the side lobe starts to increase, when it reaches to $-13.0$ dB, maximum radiation intensity decreased to $-3.0$ dB, beam width also increases; Fig. 9(b) exhibits the beam scanning properties at H-plane, from which beam scans from $0°$ to $42°$ in $yOz$ plane, with the scanning angle increasing from center of H-plane $\theta = 30°$, the side lobe also increases, when the scanning angle reaches to $\theta = 0°$, maximum radiation intensity decreased to $-3.0$ dB, however the beam width decrease and side lobe increase to $-10.0$ dB due to the asymmetric position of feed antenna, and when the scanning angle reaches $\theta = 42°$, the maximum radiation intensity decrease to $-3.0$ dB, side lobe increase to $-10.0$ dB, beam width increases.

## IV. CONCLUSION

A development of LC RA unit of 2-finger with discrete ground and a DC bias scheme of orthogonal bias electrodes reconfigurable LC RA are proposed in this article. The updated 2-finger LC RA element can achieve phase change greater than $360°$ and reflection magnitude is larger than $-2.2$ dB. Make full use of liquid crystal molecule's motion states consisting of the tilt and splay in three-dimensional space, the phase of LC RA can be controlled at 2 directions by orthogonal bias voltages. Further, steering the aperture phase on LC RA is possible, beam at both E-plane and H-plane can be steered. A pyramid horn antenna working at Ka band is used as the primary feed, $10 \times 10$-elements LC RA is designed, Radiation pattern is calculated by array synthesis with element radiation properties, phase and magnitude of RA element are obtained according to the respond results by full wave simulation. At 37.5 GHz, the LC RA can achieve beam scan at 2 orthogonal directions: scan at E-plane from $-30°$ to $30°$; H-plane from $0°$ to $42°$.

## ACKNOWLEDGMENT

The authors would like to thank Fujisawa of Tohoku University, Japan, for the information and knowledge of liquid crystal properties.

## REFERENCES

[1] D. M. Pozar, S. D. Targonski, and R. Pokuls, "A shaped-beam microstrip patch reflectarray," *IEEE Trans. Antennas Propag.*, vol. 47, no. 7, pp. 1167–1173, Jul. 1999.

[2] Y. Hou, Y. Li, and Z. Zhang, "Subwavelength and low-profile element using metallic hole for reflected antenna array," *Electron. Lett.*, vol. 55, no. 8, pp. 436–438, Apr. 2019.

[3] J. Ren and W. Menzel, "Folded reflectarray antennas based on diagonal slots patches," in *Proc. Int. Appl. Comput. Electromagn. Soc. Symp. (ACES)*, Suzhou, China, Aug. 2017, pp. 1–2.

[4] W. Yang, Q. Meng, W. Che, L. Gu, and Q. Xue, "Low-profile wideband dual-circularly polarized metasurface antenna array with large beamwidth," *IEEE Antennas Wireless Propag. Lett.*, vol. 17, no. 9, pp. 1613–1616, Sep. 2018.

[5] S. Liu and Q. Chen, "A wideband, multifunctional reflect-transmit-array antenna with polarization-dependent operation," *IEEE Trans. Antennas Propag.*, vol. 69, no. 3, pp. 1383–1392, Mar. 2021.

[6] S. Liu, H. Sato, and Q. Chen, "A wideband, 1 bit transmitarray antenna design with flat gain response," *IEEE Trans. Antennas Propag.*, vol. 68, no. 10, pp. 7046–7055, Oct. 2020.

[7] X. Tan, Z. Sun, J. M. Jornet, and D. Pados, "Increasing indoor spectrum sharing capacity using smart reflect-array," in *Proc. IEEE Int. Conf. Commun. (ICC)*, Kuala Lumpur, Malaysia, May 2016, pp. 1–6.

[8] M. Riel and J.-J. Laurin, "Design of an electronically beam scanning reflectarray using aperture-coupled elements," *IEEE Trans. Antennas Propag.*, vol. 55, no. 5, pp. 1260–1266, May 2007.

[9] H. L. Southall and D. T. McGrath, "An experimental completely overlapped subarray antenna," *IEEE Trans. Antennas Propag.*, vol. 34, no. 4, pp. 465–474, Apr. 1986.

[10] S.-H. Hsu, C. Han, J. Huang, and K. Chang, "An offset linear-array-fed Ku/Ka dual-band reflectarray for planet cloud/precipitation radar," *IEEE Trans. Antennas Propag.*, vol. 55, no. 11, pp. 3114–3122, Nov. 2007.

[11] P. Nayeri, F. Yang, and A. Z. Elsherbeni, "Beam-scanning reflectarray antennas: A technical overview and state of the art," *IEEE Antennas Propag. Mag.*, vol. 57, no. 4, pp. 32–47, Aug. 2015.

[12] J. Huang and R. J. Pogorzelski, "A Ka-band microstrip reflectarray with elements having variable rotation angles," *IEEE Trans. Antennas Propag.*, vol. 46, no. 5, pp. 650–656, May 1998.

[13] M. Wang, S. Xu, F. Yang, and M. Li, "A 1-bit bidirectional reconfigurable transmit-reflect-array using a single-layer slot element with PIN diodes," *IEEE Trans. Antennas Propag.*, vol. 67, no. 9, pp. 6205–6210, Sep. 2019.

[14] J. Perruisseau-Carrier, F. Bongard, R. Golubovic-Niciforovic, R. Torres-Sánchez, and J. R. Mosig, "Contributions to the modeling and design of reconfigurable reflecting cells embedding discrete control elements," *IEEE Trans. Microw. Theory Techn.*, vol. 58, no. 6, pp. 1621–1628, Jun. 2010.

[15] O. Bayraktar, O. A. Civi, and T. Akin, "Beam switching reflectarray monolithically integrated with RF MEMS switches," *IEEE Trans. Antennas Propag.*, vol. 60, no. 2, pp. 854–862, Feb. 2012.

[16] H. Rajagopalan, Y. Rahmat-Samii, and W. A. Imbriale, "RF MEMS actuated reconfigurable reflectarray patch-slot element," *IEEE Trans. Antennas Propag.*, vol. 56, no. 12, pp. 3689–3699, Dec. 2008.

[17] S. V. Hum, G. McFeetors, and M. Okoniewski, "Integrated MEMS reflectarray elements," in *Proc. 1st Eur. Conf. Antennas Propag.*, Nice, France, Nov. 2006, pp. 1–6.

[18] G. Perez-Palomino, R. Florencio, J. A. Encinar, M. Barba, R. Dickie, R. Cahill, P. Baine, M. Bain, and R. R. Boix, "Accurate and efficient modeling to calculate the voltage dependence of liquid crystal-based reflectarray cells," *IEEE Trans. Antennas Propag.*, vol. 62, no. 5, pp. 2659–2668, May 2014.

[19] G. Perez-Palomino, M. Barba, J. A. Encinar, R. Cahill, R. Dickie, P. Baine, and M. Bain, "Design and demonstration of an electronically scanned reflectarray antenna at 100 GHz using multiresonant cells based on liquid crystals," *IEEE Trans. Antennas Propag.*, vol. 63, no. 8, pp. 3722–3727, Aug. 2015.

[20] G. Perez-Palomino, P. Baine, R. Dickie, M. Bain, J. A. Encinar, R. Cahill, M. Barba, and G. Toso, "Design and experimental validation of liquid crystal-based reconfigurable reflectarray elements with improved bandwidth in F-band," *IEEE Trans. Antennas Propag.*, vol. 61, no. 4, pp. 1704–1713, Apr. 2013.

[21] W. Hu, R. Cahill, J. A. Encinar, R. Dickie, H. Gamble,V. Fusco, and N. Grant, "Design and measurement of reconfigurable millimeter wave reflectarray cells with nematic liquid crystal," *IEEE Trans. Antennas Propag.*, vol. 56, no. 10, pp. 3112–3117, Oct. 2008.

[22] S.-Y. Sun, X. Yu, P.-J. Wang, C.-F. Wan, J. Yang, Z. Yin, G. Deng, and H.-B. Lu, "Electronically tunable liquid-crystal-based F-band phase shifter," *IEEE Access*, vol. 8, pp. 151065–151071, 2020.

[23] J. Yang, X. Chu, H. Gao, P. Wang, G. Deng, Z. Yin, and H. Lu, "Fully electronically phase modulation of millimeter-wave via comb electrodes and liquid crystal," *IEEE Antennas Wireless Propag. Lett.*, vol. 20, no. 3, pp. 342–345, Mar. 2021.

[24] S. Bildik, S. Dieter, C. Fritzsch, W. Menzel, and R. Jakoby, "Reconfigurable folded reflectarray antenna based upon liquid crystal technology," *IEEE Trans. Antennas Propag.*, vol. 63, no. 1, pp. 122–132, Jan. 2015.

[25] S. Bildik, S. Dieter, C. Fritzsch, M. Frei, C. Fischer, W. Menzel, and R. Jakoby, "Reconfigurable liquid crystal reflectarray with extended tunable phase range," in *Proc. 41st Eur. Microw. Conf.*, Manchester, U.K., Oct. 2011, pp. 1292–1295.

[26] D. Jiang, X. Li, Z. Fu, P. Ran, G. Wang, Z. Zheng, T. Zhang, and W.-Q. Wang, "Liquid crystal-based wideband reconfigurable leaky wave X-band antenna," *IEEE Access*, vol. 7, pp. 127320–127326, 2019.
[27] J. S. Gibson, X. Liu, S. V. Georgakopoulos, J. J. Wie, T. H. Ware, and T. J. White, "Reconfigurable antennas based on self-morphing liquid crystalline elastomers," *IEEE Access*, vol. 4, pp. 2340–2348, 2016.
[28] J. Shu, Y. Zhang, and Z. Zheng, "A novel beam steerable antenna employing tunable high impedance surface with liquid crystal," *IEEE Access*, vol. 8, pp. 118687–118695, 2020.
[29] G. Xu, H.-L. Peng, C. Sun, J.-G. Lu, Y. Zhang, and W.-Y. Yin, "Differential probe fed liquid crystal-based frequency tunable circular ring patch antenna," *IEEE Access*, vol. 6, pp. 3051–3058, 2018.
[30] P. Yaghmaee, O. H. Karabey, B. Bates, C. Fumeaux, and R. Jakoby, "Electrically tuned microwave devices using liquid crystal technology," *Int. J. Antennas Propag.*, vol. 2013, Nov. 2013, Art. no. 824214.
[31] E. Doumanis, G. Goussetis, R. Dickie, R. Cahill, P. Baine, M. Bain, V. Fusco, J. A. Encinar, and G. Toso, "Electronically reconfigurable liquid crystal based mm-Wave polarization converter," *IEEE Trans. Antennas Propag.*, vol. 62, no. 4, pp. 2302–2307, Apr. 2014.
[32] A. Moessinger, R. Marin, S. Mueller, J. Freese, and R. Jakoby, "Electronically reconfigurable reflectarrays with nematic liquid crystals," *Electron. Lett.*, vol. 42, no. 16, pp. 899–900, Aug. 2006.
[33] A. Gaebler, A. Moessinger, F. Goelden, A. Manabe, M. Goebel, R. Follmann, D. Koether, C. Modes, A. Kipka, M. Deckelmann, T. Rabe, B. Schulz, P. Kuchenbecker, A. Lapanik, S. Mueller, W. Haase, and R. Jakoby, "Liquid crystal-reconfigurable antenna concepts for space applications at microwave and millimeter waves," *Int. J. Antennas Propag.*, vol. 2009, Mar. 2009, Art. no. 876989.
[34] J. Kim and J. Oh, "Liquid-crystal-embedded aperture-coupled microstrip antenna for 5G applications," *IEEE Antennas Wireless Propag. Lett.*, vol. 19, no. 11, pp. 1958–1962, Nov. 2020.
[35] X. Li, Y. Wan, J. Liu, D. Jiang, T. Bai, K. Zhu, J. Zhuang, and W.-Q. Wang, "Broadband electronically scanned reflectarray antenna with liquid crystals," *IEEE Antennas Wireless Propag. Lett.*, vol. 20, no. 3, pp. 396–400, Mar. 2021.
[36] J. Li, T. Jin, D. Erni, F. Meng, Q. Wu, and W. Li, "Design and numerical demonstration of a 2D millimeter-wave beam-scanning reflectarray based on liquid crystals and a static driving technique," *J. Phys. D, Appl. Phys.*, vol. 52, no. 27, May 2019, Art. no. 275103.
[37] P. Deo, D. Mirshekar-Syahkal, L. Seddon, S. E. Day, and F. A. Fernández, "Microstrip device for broadband (15–65 GHz) measurement of dielectric properties of nematic liquid crystals," *IEEE Trans. Microw. Theory Techn.*, vol. 63, no. 4, pp. 1388–1398, Apr. 2015.
[38] H. Yang, F. Yang, S. Xu, Y. Mao, M. Li, X. Cao, and J. Gao, "A 1-bit $10\times10$ reconfigurable reflectarray antenna: Design, optimization, and experiment," *IEEE Trans. Antennas Propag.*, vol. 64, no. 6, pp. 2246–2254, Jun. 2016.

**XIAOTONG LI** (Student Member, IEEE) received the B.E. degree from the Agricultural University of Hebei, Baoding, China, in 2014, and the M.E. degree from Xidian University, Xi'an, China, in 2017. He is currently pursuing the Ph.D. degree with the Department of Communications Engineering, Tohoku University, Sendai, Japan.

His current research interests include computational electromagnetic, method of moments, reflectarray antennas, reconfigurable antennas, and periodic structures.

**HIROYASU SATO** (Member, IEEE) received the B.E. and M.E. degrees from Chuo University, Tokyo, Japan, in 1993 and 1995, respectively, and the D.E. degree from Tohoku University, Sendai, Japan, in 1998. He is currently an Assistant Professor with the Department of Communications Engineering, Tohoku University. His current research interests include the experimental study of electromagnetic waves, computational electromagnetics, antennas in plasma, antennas for plasma production, broadband antennas, wireless power transfer, and active/passive millimeter wave imaging. He is a member of the Institute of Electronics, Information and Communication Engineers (IEICE). He received the First Place of the Best Paper Award from the International Symposium on Antennas and Propagation (ISAP), in 2017.

**YOSEI SHIBATA** received the Ph.D. degree in engineering from the Tokyo Institute of Technology, Japan, in March 2013. Then, he joined the National Institute of Advanced Industrial Science and Technologies (AIST), Japan, as a Postdoctoral Researcher. In October 2015, he joined the Department of Electronics, Tohoku University, as an Assistant Professor. His research interests include control of molecular ordering and its device applications. He received the M&BE7 Student Poster Award, in 2013, the JSAP Young Scientist Presentation Award, in 2015, the ITE Frontier Award, in 2019, the JLCS Young Researcher's Award, in 2020, and the Tokin-Foundation Industrial Achievement Award, in 2021.

**TAKAHIRO ISHINABE** (Member, IEEE) received the B.S., M.S., and Ph.D. degrees in electronic engineering from Tohoku University, Sendai, Japan, in 1995, 1997, and 2000, respectively. From 2000 to 2002, he was a Research Fellow of the Japan Society for the Promotion of Science, and from 2003 to 2012, he was an Assistant Professor. Since 2013, he has been an Associate Professor with the Department of Electronics, Graduate School of Engineering, Tohoku University. He was also a Visiting Professor with the CREOL, The College of Optics and Photonics, University of Central Florida, from 2010 to 2011. He has been performing a research on advanced liquid crystal displays, such as wide viewing angle LCD, reflective full-color LCD, field sequential color LCD, and flexible LCD. He has been a fellow of Society for Information Display, since 2020.

**HIDEO FUJIKAKE** (Senior Member, IEEE) received the M.E. and Ph.D. degrees from Tohoku University, Japan, in 1985 and 2003, respectively. In 1985, he joined Japan Broadcasting Corporation (NHK). In 1988 and 2012, he was with the NHK Science and Technology Research Laboratories. Since 2012, he has been a Professor with the Department of Electronic Engineering, Tohoku University. His current research interests include flexible liquid crystal displays, optical functional liquid crystal devices, and liquid crystal materials for high frequency electromagnetic wave communications.

He has been an IEICE Fellow, since 2015, an ITE Fellow, since 2016, and a Japan Society of Applied Physics (JSAP) Fellow, since 2019. He received the Best Paper Award from the Institute of Electronics, Information and Communication Engineers (IEICE), in 2001 and 2017, the Best Paper Award from Japanese Liquid Crystal Society (JLCS), in 2001 and 2015, the Niwa-Takayanagi Best Paper Awards from the Institute of Image Information and Television Engineers of Japan (ITE), in 2003 and 2009, and the Electronics Society Award from IEICE, in 2013. He also served as the General Vice-Chair for International Display Workshops, in 2015 and 2016, the Japan Chapter Chair for IEEE Consumer Electronics Society, in 2012 and 2014, and the Vice President of Japanese Liquid Crystal Society, in 2015 and 2016.

**QIANG CHEN** (Senior Member, IEEE) received the B.E. degree from Xidian University, Xi'an, China, in 1986, and the M.E. and D.E. degrees from Tohoku University, Sendai, Japan, in 1991 and 1994, respectively. He is currently a Chair Professor with the Electromagnetic Engineering Laboratory, Department of Communications Engineering, Faculty of Engineering, Tohoku University. His research interests include antennas, microwave and millimeter wave, electromagnetic measurement, and computational electromagnetics. He is an IEICE Fellow. He received the Best Paper Award and Zen-Ichi Kiyasu Award from the Institute of Electronics, Information and Communication Engineers (IEICE), in 2009. He served as the Chair for IEICE Technical Committee on Photonics-Applied Electromagnetic Measurement, from 2012 to 2014, the Chair for IEICE Technical Committee on Wireless Power Transfer, from 2016 to 2018, and the Chair for IEEE Antennas and Propagation Society Tokyo Chapter, from 2017 to 2018. He is currently the Chair of IEICE Technical Committee on Antennas and Propagation.